Topological Hall effect induced by classical large-spin background: $su(2)$ path-integral approach

Kaushal K. Kesharpu ⓘ,[1,*] Evgenii A. Kochetov,[1] and Alvaro Ferraz[2]

[1]*Bogoliubov Laboratory of Theoretical Physics, Joint Institute for Nuclear Research, Dubna, Moscow Region 141980, Russia*
[2]*International Institute of Physics - UFRN, Department of Experimental and Theoretical Physics - UFRN, Natal 59078-970, Brazil*

The $su(2)$ coherent-state path-integral technique is employed to study lattice electrons strongly coupled to a quantum spin background. In the large-spin limit it is replaced by its classical counterpart that breaks the time-reversal symmetry. The fermions propagating through a classical large-spin texture may then exhibit the topological Hall effect which arises even for a zero scalar spin chirality of the underlying spin background.

I. INTRODUCTION

The topological Hall effect (THE) may be viewed as arising from the electron hopping in a classical spin background that breaks time-reversal symmetry. This results in the anomalous Hall conductivity in the absence of any externally applied magnetic field. The THE attracts attention from both physics and engineering communities due to the novel physics it contains and due to the potential applications to electronics and spintronics. The simplest examples come from a mean-field treatment of the Kondo-lattice interaction (the double exchange model) of the itinerant electrons and the classical localized spins that form noncoplanar spin textures [1–4].

Specifically, one starts with the simplest lattice Kondo-type model of the tight-binding electrons strongly coupled to the localized spins $\hat{\mathbf{S}}_i$ described by the Hamiltonian

$$H = -\sum_{ij\sigma}\left(t_{ij} + \frac{3J}{4}\delta_{ij}\right)c_{i\sigma}^\dagger c_{j\sigma} + J\sum_i \hat{\mathbf{S}}_i \cdot (c_{i\sigma}^\dagger \vec{\sigma}_{\sigma\sigma'}c_{i\sigma'}).$$

(1)

Here, $c_{i\sigma}^\dagger$ creates an electron with the spin σ on site i. $J > 0$ stands for the exchange coupling constant. $\vec{\sigma}$ is the vector of the Pauli spin matrices. The external magnetic moments $\hat{\mathbf{S}}_i$ are the generators of the $su(2)$ algebra in the lowest ($s = 1/2$) representation. The hopping term is modified by adding an extra J-dependent term to guarantee a finite $J \to +\infty$ limit [5]. Within a mean-field treatment the spatial spin structure is encoded in $\langle\hat{\mathbf{S}}_i\rangle = S \cdot \vec{n}_i$. Here, S is a localized spin magnitude, whereas a classical static vector $\vec{n}_i$ determines a varying direction of the localized spin.

The underlying topological spin structures can be composed of multiple spin density waves. The scalar spin chirality in the ground state due to spins of the l, m, and nth site is found by the triple product $\langle\vec{S}_l \cdot \vec{S}_m \times \vec{S}_n\rangle$. For nonzero spin chirality, the time-reversal and parity symmetries are broken. Hence, when conduction electrons propagate through such a spin texture, due to the accumulation of the Berry phase, the system may show THE [6]. Typical postulated spin textures are

chiral stripes, spiral spin configurations, and skyrmion spin structures [7,8]. In particular, the experimentally observed skyrmion lattice can be viewed as a lattice of topologically stable knots in the underlying spin structure [9,10].

Away from the mean-field treatment one should consider operators $\hat{\mathbf{S}}_i$ for $S > 1/2$ as being the generators of the higher spin-S representation, which poses a technical problem. On the other hand, the $su(2)$ coherent-state (CS) path integral incorporates S just as a parameter [11]. The CS integral is entirely determined by the $su(2)$ algebra commutation relations that do not depend on a chosen representation. It therefore seems appropriate to alternatively treat the problem in terms of the CS path-integral representation for the partition function. In this way one avoids explicit matrix representations of the high-spin quantum generators, and instead deals with a compact and simple $su(2)$ path integral for the partition function. Of course by postulating the underlying spin texture as a static site-dependent field we arrive again at this stage (after the limit $J \to \infty$ is taken) in a new mean-field approximation.

In our previous work [12], we proposed such a theory to treat the THE based on the lowest $s = 1/2$ representation of the $su(2)$ algebra. The aim of this present work is twofold. First, we generalize our approach to study large-spin classical textures. This is important as that seems to be the case in many theoretical and experimental studies [6,13,14]. Second, until recently, most investigations have been focused on magnetic states with a finite spin chirality. We show that the THE does not necessarily require a nonzero scalar spin chirality. Although in the physical community it is widely believed that THE is absent for zero spin chirality [15], recent experiments have shown otherwise [16–20].

Recently, the THE in magnets having a trivial magnetic structure has been attracting broad interest. For example, a large magnitude of the crystal THE is proposed in a room-temperature collinear antiferromagnet RuO_2. Namely, if the crystal symmetry is low enough, the THE can emerge even when the background spin texture is trivial [21]. It is possible to have the THE in a noncollinear antiferromagnet with zero net magnetization. In this respect, the topological order indeed survives in the magnetic material Mn_3Ir to very high temperatures [22]. The THE is also shown to emerge in

*kesharpu@theor.jinr.ru

noncollinear spiral spin textures in a two-dimensional (2D) magnetic Rashba model [23,24]. In the present paper, we show that spin-orbit coupling is not truly a necessary ingredient for the realization of the THE exhibiting a trivial magnetic structure. It can instead be driven by time-reversal symmetry breaking in a system of strongly correlated electrons that exhibits zero spin chirality.

II. THEORETICAL FRAMEWORK

A low-energy effective theory to describe the electrons coupled to a spin-S background can be derived under the requirement that the spin background should affect the fermion hopping in such a way that the $SU(2)$ global symmetry remains intact. The electron hopping is then affected by the $su(2)$ CS overlap factor. This is analogous to the Peierls factor arising due to an external magnetic field. It is frequently referred to as the vector potential generated by a noncollinear spin texture [15]. Physically, one can view it as a fictitious magnetic field that produces a flux through an elementary plaquette. The precise meaning of that emergent artificial gauge field is as follows. It is generated by the $U(1)$ local connection one-form of the spin $U(1)$ complex line bundle. Such a construction provides a covariant (geometric) quantization of a spin [25]. In this approach the underlying base space appears as a classical spin phase space, a two-sphere S^2. It can be thought of as a complex projective space CP^1, endowed with a set of local coordinates $(z, \bar{z})$. Quantum spin is then represented as the sections $|z\rangle$ of the principle (monopole) line bundle $P(CP^1, U(1))$. The local connections of this bundle read $a^{(0)} = i\langle z|d|z\rangle$, with d standing for an exterior derivative.

This approach proves effective in studying strongly correlated electrons. This can be seen as follows. At infinitely large Kondo coupling J, Eq. (1) goes over into the $U = \infty$ Hubbard model Hamiltonian [5],

$$H_{U=\infty} = -\sum_{ij\sigma} t_{ij} \tilde{c}_{i\sigma}^\dagger \tilde{c}_{j\sigma}. \tag{2}$$

The constrained electron operator $\tilde{c}_{i\sigma} = c_{i\sigma}(1 - n_{i\bar{\sigma}})$, where $n_{i\sigma} = c_{i\sigma}^\dagger c_{i\sigma}$ is the number operator, can be dynamically (in the effective action) factorized into the spinless charged fermionic f_i fields and the spinful bosonic z_i fields [12]. Inasmuch as $f_i^2 \equiv 0$, the local no double occupancy constraint that incorporates the strong electron correlations is rigorously implemented in this representation.

The high-spin extension of the present theory can be obtained by simply generalizing the CS in the fundamental $S = 1/2$ representation for a given spin-S,

$$|z\rangle = (1 + |z|^2)^{-S} e^{z\hat{S}^-} |S\rangle, \tag{3}$$

where $|S\rangle$ represents the spin-S highest weight $su(2)$ state, and the operator $\hat{S}^-$ denotes a conventional spin lowering operator. As a result the S-dependent partition function takes on the form

$$Z = \int D\mu(z, f) \exp \mathcal{A}. \tag{4}$$

Here, the measure $D\mu(z, f)$ is defined as

$$D\mu(z, f) = \prod_{i,t} \frac{2S}{2\pi i} \frac{d\bar{z}_i(t) dz_i(t)}{(1 + |z_i|^2)^2} d\bar{f}_i(t) df_i(t). \tag{5}$$

In Eq. (5) z_i is a complex number that keeps track of the spin degrees of freedom, while f_i is a Grassmann variable that describes the charge degrees of freedom.

The effective action $\mathcal{A}$ in Eq. (4) is defined as

$$\mathcal{A} = \sum_i \int_0^\beta \left[ia_i^{(0)} - \bar{f}_i(\partial_t + ia_i^{(0)})f_i \right] dt - \int_0^\beta H dt. \tag{6}$$

It involves the $u(1)$-valued connection one-form of the magnetic monopole bundle that can formally be interpreted as a spin kinetic term

$$ia^{(0)} = -\langle z|\partial_t|z\rangle = S\frac{\dot{\bar{z}}z - \bar{z}\dot{z}}{1 + |z|^2}, \tag{7}$$

which can be identified as the Berry connection. The dynamical part of the action can be written as

$$H = -t \sum_{ij} \bar{f}_i f_j e^{ia_{ji}} + \text{H.c.} + \mu \sum_i \bar{f}_i f_i. \tag{8}$$

Here,

$$a_{ij} = -i\log\langle z_i|z_j\rangle, \quad \langle z_i|z_j\rangle = \frac{(1 + \bar{z}_i z_j)^{2S}}{(1 + |z_j|^2)^S (1 + |z_i|^2)^S}.$$

The hopping term in Eq. (8) is affected by the $su(2)$ coherent-state overlap factor in the S representation. The modulus of this factor

$$|\langle z_i|z_j\rangle| = \left[\frac{(1 + \bar{z}_i z_j)(1 + \bar{z}_j z_i)}{(1 + |z_i|^2)(1 + |z_j|^2)} \right]^S =: \rho_{ij}^S. \tag{9}$$

Here, $\rho_{ij} \in [0, 1]$. The hopping probability is reduced by the presence of a factor ρ_{ij}^S which is proportional to the overlap of the spin-wave functions on neighboring sites. In the limiting ferromagnetic (FM) case ($z_i = z_j$) those wave functions are identical and $\rho = 1$ at any spin value S. There is no overlap in the antiferromagnetic (AFM) case ($z_j = -1/z_i$) at any S, hence $\rho = 0$. The hopping creates changes in the spin configuration, unless the spin polarization is uniform. The growing S inhibits the hopping by reducing the spin-wave function overlap. As a result, away from the FM case as $\rho_{ij} < 1$, and, eventually, with increasing $S \to \infty$, $\rho_{ij}^S \to 0$. This is the expected physical behavior in such a regime [26].

The passage from Eq. (1) to Eq. (8) implies that we take the limit $J/t \to \infty$ keeping at the same time the $su(2)$ spin generators $\hat{S}_i$ fixed. In this limit the quantum local spins are fully screened and cannot be replaced by fixed classical values. The spin classical limit implies instead that we replace from the very beginning $\hat{S}_i$ in Eq. (1) by the c-numbers $S\langle \bar{n}_i \rangle$. This fully ignores quantum Kondo screening [27].

Under a global $SU(2)$ rotation

$$z_i \to \frac{uz_i + v}{-\bar{v}z_i + \bar{u}}, \tag{10}$$

the phase will be

$$a_i^{(0)} \to a_i^{(0)} - \partial_t\theta_i, \quad a_{ij} \to a_{ij} + \theta_j - \theta_i, \tag{11}$$

where

$$\theta_i = iS \log \left(\frac{v\bar{z}_i + u}{\bar{v}z_i + \bar{u}} \right), \quad \begin{pmatrix} u & v \\ -\bar{v} & \bar{u} \end{pmatrix} \in SU(2). \quad (12)$$

One can clearly observe that the effective action $\mathcal{A}$ remains invariant under $SU(2)$ transformations, provided the fermionic operators are $U(1)$ transformed as

$$f_i \rightarrow e^{i\theta_i} f_i. \quad (13)$$

A flux through a plaquette $\sum_{\text{plaq}} a_{ij}$ generated by the $SU(2)$ transformation remains invariant under Eq. (11).

By definition the phase a_{ji} in Eq. (8) is a complex valued function. Hence, the real and imaginary parts of a_{ij} are

$$a_{ji} = \phi_{ji} + i\chi_{ji}, \quad \bar{\phi}_{ji} = \phi_{ji}, \quad \bar{\chi}_{ji} = \chi_{ji}. \quad (14)$$

The ϕ_{ji} and χ_{ji} are defined as [28]

$$
\begin{aligned}
\phi_{ji} &= iS \log \frac{1 + \bar{z}_i z_j}{1 + \bar{z}_j z_i} \\
&= iS \log \frac{(S + S_i^z)(S + S_j^z) + S_i^- S_j^+}{(S + S_i^z)(S + S_j^z) + S_j^- S_i^+}, \\
\chi_{ji} &= -S \log \frac{(1 + \bar{z}_i z_j)(1 + \bar{z}_j z_i)}{(1 + |z_i|^2)(1 + |z_j|^2)} \\
&= -S \log \left(\frac{\vec{S}_i \cdot \vec{S}_j}{2S^2} + \frac{1}{2} \right). \quad (15)
\end{aligned}
$$

Using Eq. (15) it can be checked that, under a $SU(2)$ global rotation, χ_{ji} remains intact, however, ϕ_{ji} transforms as

$$\phi_{ji} \rightarrow \phi_{ji} + \theta_i - \theta_j. \quad (16)$$

This transformation appears as a gauge fixing by choosing a specific rotational covariant frame. The dynamical fluxes do not depend on that choice.

The potentials $\phi_i^{(0)} := ia_i^{(0)}$ and ϕ_{ji} formally remind those gauge fields that define a compact $U(1)$ lattice gauge theory. This is due to the fact that both theories are formulated as $U(1)$ complex line bundles. The gauge potentials (local connections in these bundles) in both theories transform formally in the same way under a change in the local trivialization [29]. In our case, the different trivializing coverings of the spin base manifold S^2 are related to each other through the global $SU(2)$ rotations [Eq. (10)].

III. TOPOLOGY

Using Eq. (15) the Hamiltonian can be explicitly written as

$$H = -t \sum_{\langle i,j \rangle} \bar{f}_i f_j e^{i\phi_{ji}} \left(\frac{\vec{S}_i \cdot \vec{S}_j}{2S^2} + \frac{1}{2} \right)^S + \mu \sum_i \bar{f}_i f_i. \quad (17)$$

Physically, it represents the interaction between an underlying spin texture and the itinerant spinless fermions. When $S = 1/2$ this Hamiltonian reduces to that derived in Ref. [12]. Here, we generalize our approach to large values of spin $S \gg 1/2$. After all, the classical treatment of the underlying

spin structure is more justifiable when S is larger than the electronic spin.

We take a two-band system having opposite Chern number. Physically, one can consider a bipartite two-dimensional (2D) lattice L, consisting of two sublattices A and B; $L = A \oplus B$. If on sublattice A the charge and spin degrees of freedom are f_i and z_i, respectively, then for convenience on sublattice B they are defined as

$$f_i \rightarrow f_i e^{i\theta_i^{(0)}}, \quad z_i \rightarrow -\frac{1}{\bar{z}_i}, \quad i \in B. \quad (18)$$

Here, $\theta_i^{(0)} \equiv \theta_i|_{u=0, v=1}$ in Eq. (12). Under these transformations the χ_{ji} remains unchanged while $\phi_{ji} \rightarrow \phi_{ij} + \theta_j^{(0)} - \theta_i^{(0)}$. Also, the CS image of the on-site electron spin operators changes sign, $\vec{S}_i \rightarrow -\vec{S}_i$. As $\phi_{ji} = -\phi_{ij}$, we see that the phases of the hopping factors corresponding to the A and B sublattices are opposite in sign. This means that the dynamical fluxes piercing through elementary plaquettes that compose a unit cell are opposite in sign. Fixing them as classical c-numbers breaks time-reversal symmetry. Indeed, they are analogous to the homogeneous c-valued phase factors in the next-nearest-neighbor (NNN) hopping, $t_2 \rightarrow t_2 e^{\pm i\phi}$, introduced by Haldane [30]. Hence, as in the Haldane model, one can expect a nonzero Hall effect emerging due to the resulting time-reversal symmetry breaking. It should be noted that the time-reversal symmetry in the Haldane model was broken by inserting nonzero local fluxes, with the summation of those fluxes over the unit cell being zero. In contrast, in our model Eq. (8) we simply break time-reversal symmetry by fixing the spin connection term a_{ij} as a classical static quantity. In fact, fixing the a_{ij} may result in breaking time reversal even for zero spin chirality.

A. An example: Conical spin configuration

Below we take a simple spin configuration to illustrate our approach. Interestingly, this spin structure shows a nontrivial topological effect, although its scalar spin chirality is zero. The spin-S field is defined as

$$\vec{S}_i = (S_i^x, S_i^y, S_i^z) \equiv (\epsilon \cos \vec{q} \cdot \vec{r}_i, \epsilon \sin \vec{q} \cdot \vec{r}_i, \sqrt{S^2 - \epsilon^2}). \quad (19)$$

Here, $\vec{S}_i$ is the spin at the ith site, $\vec{q}$ is the spin modulation vector, and $\vec{r}_i$ is the position vector, with S being some arbitrary constant spin value, and ϵ some small parameter satisfying $\epsilon \ll S$. Physically, it represents the precession of spin S around the z axis with a constant azimuthal angle $\pi/2 - \arctan(\sqrt{S^2 - \epsilon^2}/\epsilon)$. This formalism is applicable to a thin film or to a surface of a multiferroic single crystal assuming a constant $|\vec{S}_i| = S$ [31]. Keeping the terms only up to second order in ϵ, the hopping term contributions of the Hamiltonian [Eq. (17)] only for sublattice A are

$$
\begin{aligned}
e^{-\chi_{ij}} &\approx 1 - \frac{\epsilon^2}{S} \sin^2 \frac{\vec{q} \cdot \vec{r}_{ij}}{2}, \\
e^{i\phi_{ji}} &\approx \exp \left(i \frac{\epsilon^2}{2S} \sin \vec{q} \cdot \vec{r}_{ij} \right). \quad (20)
\end{aligned}
$$

Here, we define $\vec{r}_{ij} = \vec{r}_i - \vec{r}_j$. At sublattice B the χ_{ij} remains the same, but $\phi_{ji} \rightarrow -\phi_{ji}|_{i,j \in A} + 2S\vec{q} \cdot \vec{r}_{ij}$. Therefore

$$e^{-\chi_{ij}} \approx 1 - \frac{\epsilon^2}{S} \sin^2 \frac{\vec{q} \cdot \vec{r}_{ij}}{2}, \quad e^{i\phi_{ji}} \approx \exp\left(-i\frac{\epsilon^2}{2S} \sin \vec{q} \cdot \vec{r}_{ij} + i2S\vec{q} \cdot \vec{r}_{ij}\right). \tag{21}$$

Similarly, for interlattice hoppings ($i \in A$, $j \in B$),

$$e^{-\chi_{ij}} \approx \left(\frac{\epsilon}{S} \sin \frac{\vec{q} \cdot \vec{r}_{ij}}{2}\right)^{2S}, \quad e^{i\phi_{ji}} \approx e^{iS(\vec{q} \cdot \vec{r}_{ij} - \pi)}. \tag{22}$$

The total Hamiltonian is found by substituting Eqs. (20)–(22) in Eq. (17):

$$\begin{aligned}
H = &-t_2 \sum_{i,j \in A} \bar{f}_i f_j \left(1 + i\frac{\epsilon^2}{S} \sin \frac{\vec{q} \cdot \vec{r}_{ij}}{2} e^{i\vec{q} \cdot \vec{r}_{ij}/2}\right) e^{-iS\vec{q} \cdot \vec{r}_{ij}} - t_2 \sum_{i,j \in B} \bar{f}_i f_j \left(1 - i\frac{\epsilon^2}{S} \sin \frac{\vec{q} \cdot \vec{r}_{ij}}{2} e^{-i\vec{q} \cdot \vec{r}_{ij}/2}\right) e^{iS\vec{q} \cdot \vec{r}_{ij}} \\
&-t_1 \left(\frac{\epsilon}{S}\right)^{2S} \sum_{\substack{i \in A \\ j \in B}} \bar{f}_i f_j \left|\sin \frac{\vec{q} \cdot \vec{r}_{ij}}{2}\right|^{2S} + \text{H.c.}
\end{aligned} \tag{23}$$

It should be stressed that the $\vec{r}_{ij}$ in the first and in the second terms are different from the $\vec{r}_{ij}$ in the third term. In Eq. (23) the third term on the right-hand side is real and it corresponds to nearest-neighbor (NN) hopping contributions. The first and the second terms correspond to the NNN hopping processes and they are complex valued; in fact, they are conjugates of each other, which is a necessary condition for time-reversal symmetry breaking.

In momentum space the Hamiltonian is written as

$$H = \sum_{\vec{k}} \bar{\psi}_{\vec{k}} \mathcal{H}(\vec{k}) \psi_{\vec{k}}. \tag{24}$$

Here, $\vec{k}$ is the wave vector whose values lie only in the first Brillouin zone. The matrix $\bar{\psi}_{\vec{k}} = [\bar{f}_{\vec{k},A}, \bar{f}_{\vec{k},B}]$ contains the annihilation operators of the $\vec{k}$th momentum on the A and B sublattices. The kernel $\mathcal{H}(\vec{k})$ is [32]

$$\begin{aligned}
\mathcal{H}(\vec{k}) = &\left\{t_2 \sum_n \cos \vec{k} \cdot \vec{b}_n \left[\cos S\vec{q} \cdot \vec{b}_n - \frac{\epsilon^2}{S} \sin \frac{\vec{q} \cdot \vec{b}_n}{2} \sin \frac{(2S-1)\vec{q} \cdot \vec{b}_n}{2}\right]\right\} \cdot \mathcal{I} + \left\{t_1 \left(\frac{\epsilon}{S}\right)^{2S} \sum_n \cos \vec{k} \cdot \vec{a}_n \left|\sin \frac{\vec{q} \cdot \vec{a}_n}{2}\right|^{2S}\right\} \cdot \sigma_x \\
&+ \left\{t_1 \left(\frac{\epsilon}{S}\right)^{2S} \sum_n \sin \vec{k} \cdot \vec{a}_n \left|\sin \frac{\vec{q} \cdot \vec{a}_n}{2}\right|^{2S}\right\} \cdot \sigma_y + \left\{t_2 \sum_n \sin \vec{k} \cdot \vec{b}_n \left[\sin S\vec{q} \cdot \vec{b}_n + \frac{\epsilon^2}{S} \sin \frac{\vec{q} \cdot \vec{b}_n}{2} \cos \frac{(2S-1)\vec{q} \cdot \vec{b}_n}{2}\right]\right\} \cdot \sigma_z.
\end{aligned} \tag{25}$$

Here, $\vec{b}_n$ is the NNN, and $\vec{a}_n$ is the NN hopping lattice vectors; $\mathcal{I}$ is the 2×2 unit matrix; σ_x, σ_y, and σ_z are the Pauli matrices. One can clearly observe that the time-reversal symmetry is broken in Eq. (25), as terms corresponding to σ_z are odd in k ($\propto \sin \vec{k} \cdot \vec{b}_n$). For a bipartite honeycomb lattice the NN and the NNN lattice vectors are [see Fig. 1(b)]

$$\vec{a}_1 = \left(\frac{\sqrt{3}d}{2}, \frac{d}{2}\right), \quad \vec{a}_2 = \left(-\frac{\sqrt{3}d}{2}, \frac{d}{2}\right), \quad \vec{a}_3 = (0, d),$$

$$\vec{b}_1 = \left(-\frac{\sqrt{3}d}{2}, \frac{3d}{2}\right), \quad \vec{b}_2 = \left(-\frac{\sqrt{3}d}{2}, -\frac{3d}{2}\right),$$

$$\vec{b}_3 = (\sqrt{3}d, 0).$$

Here, d is the lattice unit length, and for simplicity we take $d = 1$. These vectors can be substituted in Eq. (25) to get the corresponding Hamiltonian. Two different cases arise for the resulting Hamiltonian: (i) $t_2 = 0$ and $\epsilon \neq 0$, (ii) $t_2 \neq 0$ and $\epsilon = 0$. For the first case the system is an insulator if the terms corresponding to σ_x and σ_y are nonzero over the Brillouin zone. However, depending on the spin-wave vector q, there can exist some special values of k for which the terms

corresponding to σ_x and to σ_y are also zero. At these special points the energy is degenerate. This degeneracy can be lifted by adding the NNN interactions ($t_2 \neq 0$). This emergent gap is protected by time-reversal symmetry breaking, because now the term corresponding to σ_z, which breaks the time-reversal symmetry, enters into the Hamiltonian. For example, if we take $\vec{q} = (2q/\sqrt{3}, 0)$, then the special points occur at $\vec{K} = (\pm \pi/\sqrt{3}, 0)$. The Chern number in this case is

$$c_1 = \text{sgn}(\sin Sq), \quad -\frac{\sqrt{3}\pi}{2} \leqslant q \leqslant \frac{\sqrt{3}\pi}{2}. \tag{26}$$

It is the first Chern character of the corresponding $U(1)$ Bloch bundle. Interestingly, the Chern number depends on the spin S and on the modulation vector $\vec{q}$.

Similarly, for the second case, $t_2 \neq 0$ and $\epsilon = 0$, the Hamiltonian will be

$$\mathcal{H}(\vec{k}) \sim \sum_n^3 \text{diag}[\cos(\vec{k} - S\vec{q}) \cdot \vec{b}_n, \cos(\vec{k} + S\vec{q}) \cdot \vec{b}_n]. \tag{27}$$

(a)   (b)

(c)   (d)

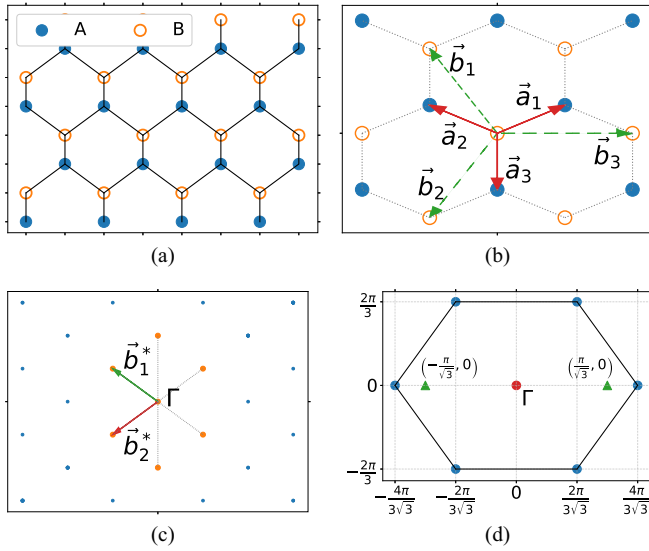FIG. 1. (a) Schematic of the honeycomb bipartite lattice with two types of atoms A and B. (b) The NN vectors $\vec{a}_1$, $\vec{a}_2$, and $\vec{a}_3$, and the NNN vectors $\vec{b}_1$, $\vec{b}_2$, and $\vec{b}_3$. (c) The reciprocal space of the honeycomb bipartite lattice. The reciprocal unit vectors are $\vec{b}_1^* = 2\pi(-\frac{1}{\sqrt{3}}, \frac{1}{3})$, $\vec{b}_2^* = 2\pi(-\frac{1}{\sqrt{3}}, -\frac{1}{3})$. (d) The first Brillouin zone of the honeycomb bipartite lattice. The special points (triangle), when terms $\sim \sigma_x$ and $\sim \sigma_y$ are zero, for $\vec{q} = (2q/\sqrt{3}, 0)$ lie at $\vec{K} = (\pm\pi/\sqrt{3}, 0)$.

By an appropriate change of the variable $\vec{k} \rightarrow \vec{k} \pm S\vec{q}$ on the A and B sublattices we will get

$$\mathcal{H}(\vec{k}) \sim \cos k_x \cos k_y. \qquad (28)$$

This Hamiltonian is time-reversal invariant, and exhibits no topological properties, as $c_1 = 0$. Physically, $\epsilon = 0$ corresponds to the ferromagnetic phase with constant spin z component. Due to the absence of the variation of the underlying spin structure the electrons do not acquire any Berry phase during hopping. Hence there is no topological effect in this case. The kth mode energy of the Hamiltonian [Eq. (25)] for the upper band is

$$E(\vec{k}) = \mathcal{H}_0(\vec{k}) + \sqrt{\mathcal{H}_x^2(\vec{k}) + \mathcal{H}_y^2(\vec{k}) + \mathcal{H}_z^2(\vec{k})}. \qquad (29)$$

The total energy of the system is established by integrating Eq. (29) over the whole Brillouin zone. Of course the resulting integral will be a function of $\vec{q}$ only. In Fig. 2 we plot the full dependence of the energy of the system on $\vec{q}$. It can be observed that for $\vec{q} = (\pm\pi/\sqrt{3}, 0)$ the energy is a minimum. Hence, for the conical spin structures in the ground state $q = \pm\pi/2$. In a honeycomb bipartite lattice every site has three nearest neighbors as shown in Fig. 3(b). Hence, the scalar spin chirality at the lth site for a honeycomb lattice can be calculated as

$$\chi_l = \sum_{(m,n)} \vec{S}_l \cdot [\vec{S}_m \times \vec{S}_n]. \qquad (30)$$

Here, (m, n) represents the even permutation of the nearest neighbors of the lth site. The total chirality is determined by summing χ_l over the whole lattice. In fact, for a honeycomb bipartite lattice the total chirality is the summation of the
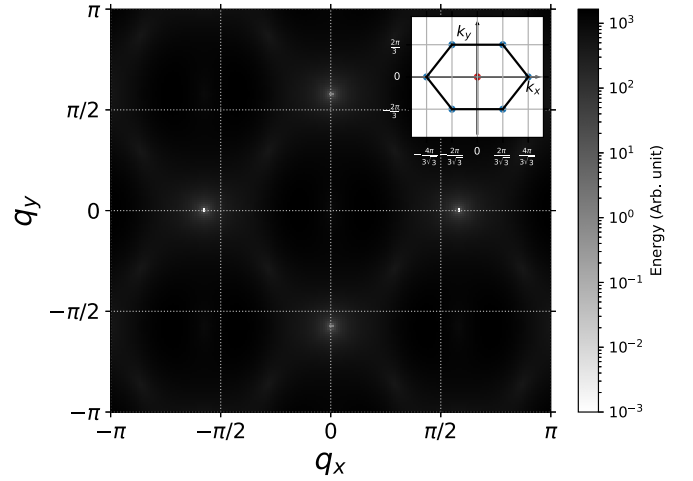

FIG. 2. Dependence of the total energy of the system on the spin modulation vector $\vec{q}$ for a conical spin configuration. The total energy is found by numerically integrating Eq. (29) over the Brillouin zone (inset). The minimum energy—the ground state—occurs at $\vec{q} = (\pm\pi/\sqrt{3}, 0)$.

chirality of sublattice A and sublattice B:

$$\chi = \sum_{l \in A} \chi_l^A + \sum_{l \in B} \chi_l^B. \qquad (31)$$

Using Eq. (30) we can calculate the chirality of the conical spin configuration for two adjacent A and B atoms connected by the NN vector $\vec{a}_3$, which is $\chi_l^A = -\chi_l^B$. Hence the total chirality will be $\chi = 0$.

As a result we arrive at the THE in spite of the zero total chirality. This is in agreement with a number of other recent
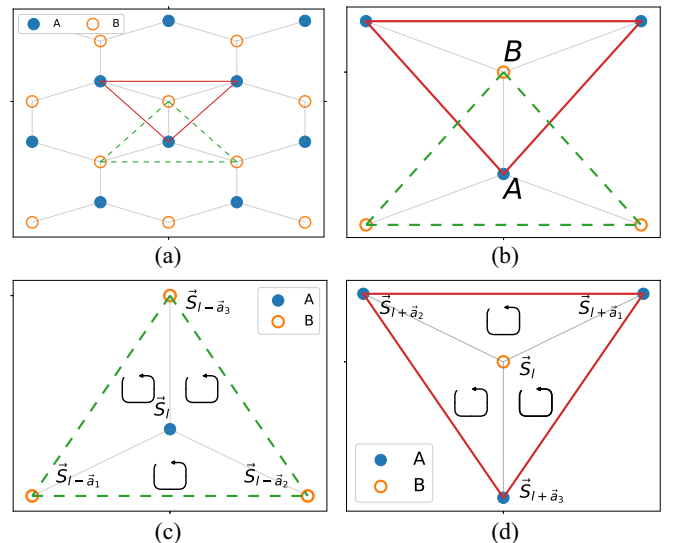

(a)   (b)

(c)   (d)

FIG. 3. (a), (b) Nearest neighbors of atoms A and B in a honeycomb bipartite lattice. Every lattice site contains three nearest neighbors. Moreover, for atom A the nearest neighbors are atom B, and vice versa. (c) Spin configuration of the atom A and its nearest neighbors. $\vec{S}_l$ represents the spin of the lth site. The chirality of the lth site is found by summing the chirality of the spin triangles: $\triangle\vec{S}_l\vec{S}_{l-\vec{a}_2}\vec{S}_{l-\vec{a}_3}$, $\triangle\vec{S}_l\vec{S}_{l-\vec{a}_3}\vec{S}_{l-\vec{a}_1}$, and $\triangle\vec{S}_l\vec{S}_{l-\vec{a}_1}\vec{S}_{l-\vec{a}_2}$. (d) Spin configuration of the atom B and its nearest neighbors.

independent results which indicate the emergence of THE even if the scalar spin chirality is identically zero [16–20,33–36]. In all of these works the THE was ascribed to the spin fluctuation as a function of the temperature [16,17,34–37]. At a higher temperature a small varying z-spin component may become manifest in the conical spin configuration. In such a case the accumulated Berry phase is nonzero and the THE emerges out of that [17,37]. However, in our model, we show that the THE state emerges even if the temperature-induced fluctuations are not present in the physical system.

IV. CONCLUSION

We show that the topological Hall effect can be placed into the context of the phenomena associated with strong electron correlation. The necessary step for that is achieved by replacing the large-spin connection by its classical counterpart to break the time-reversal symmetry. If the spin ordering opens a full gap in the charge excitation spectrum, the conditions are given for the topological Hall effect to be fully manifest. We show it can arise even in the absence of a nonzero scalar spin chirality of the underlying spin texture. Our approach demonstrates explicitly in what way a strong correlation can directly affect topology.

ACKNOWLEDGMENTS

[1] J. Ye, Y. B. Kim, A. J. Millis, B. I. Shraiman, P. Majumdar, and Z. Tešanović, Berry Phase Theory of the Anomalous Hall Effect: Application to Colossal Magnetoresistance Manganites, Phys. Rev. Lett. **83**, 3737 (1999).

[2] S. H. Chun, M. B. Salamon, Y. Lyanda-Geller, P. M. Goldbart, and P. D. Han, Magnetotransport in Manganites and the Role of Quantal Phases: Theory and Experiment, Phys. Rev. Lett. **84**, 757 (2000).

[3] K. Ohgushi, S. Murakami, and N. Nagaosa, Spin anisotropy and quantum Hall effect in the *kagomé* lattice: Chiral spin state based on a ferromagnet, Phys. Rev. B **62**, R6065 (2000).

[4] S. D. Yi, S. Onoda, N. Nagaosa, and J. H. Han, Skyrmions and anomalous Hall effect in a Dzyaloshinskii-Moriya spiral magnet, Phys. Rev. B **80**, 054416 (2009).

[5] I. Ivantsov, A. Ferraz, and E. Kochetov, Strong correlation, Bloch bundle topology, and spinless Haldane–Hubbard model, Ann. Phys. **441**, 168859 (2022).

[6] I. Martin and C. D. Batista, Itinerant Electron-Driven Chiral Magnetic Ordering and Spontaneous Quantum Hall Effect in Triangular Lattice Models, Phys. Rev. Lett. **101**, 156402 (2008).

[7] S. Hayami and Y. Motome, Charge density waves in multiple-Q spin states, Phys. Rev. B **104**, 144404 (2021).

[8] S. Hayami, Rectangular and square skyrmion crystals on a centrosymmetric square lattice with easy-axis anisotropy, Phys. Rev. B **105**, 174437 (2022).

[9] A. Neubauer, C. Pfleiderer, B. Binz, A. Rosch, R. Ritz, P. G. Niklowitz, and P. Böni, Topological Hall Effect in the *A* Phase of MnSi, Phys. Rev. Lett. **102**, 186602 (2009).

[10] J. H. Han, J. Zang, Z. Yang, J.-H. Park, and N. Nagaosa, Skyrmion lattice in a two-dimensional chiral magnet, Phys. Rev. B **82**, 094429 (2010).

[11] E. A. Kochetov, SU(2) coherent-state path integral, J. Math. Phys. **36**, 4667 (1995).

[12] A. Ferraz and E. Kochetov, Fractionalization of strongly correlated electrons as a possible route to quantum Hall effect without magnetic field, Phys. Rev. B **105**, 245128 (2022).

[13] F. L. Buessen, M. Hering, J. Reuther, and S. Trebst, Quantum Spin Liquids in Frustrated Spin-1 Diamond Antiferromagnets, Phys. Rev. Lett. **120**, 057201 (2018).

[14] J. R. Chamorro, L. Ge, J. Flynn, M. A. Subramanian, M. Mourigal, and T. M. McQueen, Frustrated spin one on a diamond lattice in NiRh$_2$O$_4$, Phys. Rev. Mater. **2**, 034404 (2018).

[15] N. Nagaosa and Y. Tokura, Topological properties and dynamics of magnetic skyrmions, Nat. Nanotechnol. **8**, 899 (2013).

[16] M. Afshar and I. I. Mazin, Spin spiral and topological Hall effect in Fe$_3$Ga$_4$, Phys. Rev. B **104**, 094418 (2021).

[17] J. H. Mendez, C. E. Ekuma, Y. Wu, B. W. Fulfer, J. C. Prestigiacomo, W. A. Shelton, M. Jarrell, J. Moreno, D. P. Young, P. W. Adams, A. Karki, R. Jin, J. Y. Chan, and J. F. DiTusa, Competing magnetic states, disorder, and the magnetic character of Fe$_3$Ga$_4$, Phys. Rev. B **91**, 144409 (2015).

[18] N. J. Ghimire, R. L. Dally, L. Poudel, D. C. Jones, D. Michel, N. T. Magar, M. Bleuel, M. A. McGuire, J. S. Jiang, J. F. Mitchell, J. W. Lynn, and I. I. Mazin, Competing magnetic phases and fluctuation-driven scalar spin chirality in the kagome metal YMn$_6$Sn$_6$, Sci. Adv. **6**, eabe2680 (2020).

[19] G. Gong, L. Xu, Y. Bai, Y. Wang, S. Yuan, Y. Liu, and Z. Tian, Large topological Hall effect near room temperature in noncollinear ferromagnet LaMn$_2$Ge$_2$ single crystal, Phys. Rev. Mater. **5**, 034405 (2021).

[20] Q. Wang, K. J. Neubauer, C. Duan, Q. Yin, S. Fujitsu, H. Hosono, F. Ye, R. Zhang, S. Chi, K. Krycka, H. Lei, and P. Dai, Field-induced topological Hall effect and double-fan spin structure with a c-axis component in the metallic kagome antiferromagnetic compound YMn$_6$Sn$_6$, Phys. Rev. B **103**, 014416 (2021).

[21] L. Šmejkal, R. González-Hernández, T. Jungwirth, and J. Sinova, Crystal time-reversal symmetry breaking and spontaneous Hall effect in collinear antiferromagnets, Sci. Adv. **6**, eaaz8809 (2020).

[22] H. Chen, Q. Niu, and A. H. MacDonald, Anomalous Hall Effect Arising from Noncollinear Antiferromagnetism, Phys. Rev. Lett. **112**, 017205 (2014).

[23] F. R. Lux, F. Freimuth, S. Blügel, and Y. Mokrousov, Chiral Hall Effect in Noncollinear Magnets from a Cyclic Cohomology Approach, Phys. Rev. Lett. **124**, 096602 (2020).

[24] J. Mochida and H. Ishizuka, Skew scattering by magnetic monopoles and anomalous Hall effect in spin-orbit coupled systems, arXiv:2211.10180.

[25] M. Stone, Supersymmetry and the quantum mechanics of spin, Nucl. Phys. B **314**, 557 (1989).

[26] R. Shankar, Holes in a quantum antiferromagnet: A formalism and some exact results, Nucl. Phys. B **330**, 433 (1990).

[27] This model is applicable for small as well as large values of the S. The only physical consequence is the decrease in the hopping probability for increasing as explained in the previous reply. We start with the model from Eq. (1) in the limit $J/t \to \infty$ with the $su(2)$ representation being fixed. This limit enforces the constraint of no double occupancy and must be taken prior to any mean-field treatment. Fixing of the representation fixes S as discussed in Eq. (3). We thus restrict ourselves with finite $S \geqslant 1/2$.

[28] The CS symbols of the spin operators $S_{cs} := \langle z | \hat{S} | z \rangle$ are

$$S_{cs}^+ = \frac{2Sz}{1 + |z|^2}, \quad S_{cs}^- = \frac{2S\bar{z}}{1 + |z|^2}, \quad S_{cs}^z = S \frac{1 - |z|^2}{1 + |z|^2}.$$

There is a one-to-one correspondence between the $su(2)$ generators and their CS symbols [38].

[29] M. Nakahara, *Geometry, Topology and Physics*, 2nd ed. (CRC Press, Boca Raton, FL, 2018).

[30] F. D. M. Haldane, Model for a Quantum Hall Effect without Landau Levels: Condensed-Matter Realization of the "Parity Anomaly", Phys. Rev. Lett. **61**, 2015 (1988).

[31] W. Chen and A. P. Schnyder, Majorana edge states in superconductor-noncollinear magnet interfaces, Phys. Rev. B **92**, 214502 (2015).

[32] $H(\vec{k})$ is a 2×2 matrix. In terms of Pauli matrices it is represented as

$$\mathcal{H}(\vec{k}) = \mathcal{H}_0 \mathcal{I} + \mathcal{H}_x(\vec{k})\sigma_x + \mathcal{H}_y(\vec{k})\sigma_y + \mathcal{H}_z(\vec{k})\sigma_z,$$

where $\quad \mathcal{H}_0(\vec{k}) = \dfrac{H_{i, j \in A} + H_{i, j \in B}}{2}, \quad \mathcal{H}_x(\vec{k}) = \text{Re}[H_{i \in A, j \in B}],$

$\mathcal{H}_z(\vec{k}) = \dfrac{H_{i, j \in A} - H_{i, j \in B}}{2}, \quad \mathcal{H}_y(\vec{k}) = \text{Im}[H_{i \in A, j \in B}].$

Here, $\mathcal{I}$ is the 2×2 unit matrix; σ_x, σ_y, and σ_z are the Pauli matrices.

[33] T. Dao, S. S. Pershoguba, and J. Zang, Hall effect induced by topologically trivial target skyrmions, arXiv:2210.11459.

[34] O. Busch, B. Göbel, and I. Mertig, Microscopic origin of the anomalous Hall effect in noncollinear kagome magnets, Phys. Rev. Res. **2**, 033112 (2020).

[35] Y. Cheng, S. Yu, M. Zhu, J. Hwang, and F. Yang, Evidence of the Topological Hall Effect in Pt/Antiferromagnetic Insulator Bilayers, Phys. Rev. Lett. **123**, 237206 (2019).

[36] W. Wang, M. W. Daniels, Z. Liao, Y. Zhao, J. Wang, G. Koster, G. Rijnders, C.-Z. Chang, D. Xiao, and W. Wu, Spin chirality fluctuation in two-dimensional ferromagnets with perpendicular magnetic anisotropy, Nat. Mater. **18**, 1054 (2019).

[37] G. Kimbell, C. Kim, W. Wu, M. Cuoco, and J. W. A. Robinson, Challenges in identifying chiral spin textures via the topological Hall effect, Commun. Mater. **3**, 19 (2022).

[38] F. A. Berezin, in *Introduction to Superanalysis*, edited by A. A. Kirillov (Springer, Dordrecht, 1987).